

Modelling the Spectral Reflectances of Sol-Gel Tin Doped Indium Oxide and Aluminum Doped Zinc Oxide Coatings

Nadine Wolf*, Daniel Gerstenlauer* and Jochen Manara*

*Bavarian Center for Applied Energy Research (ZAE Bayern), Am Hubland, 97074 Würzburg, Germany, nadine.wolf@zae.uni-wuerzburg.de

ABSTRACT

The spectral normal hemispherical reflectances of tin doped indium oxide (ITO) and aluminum doped zinc oxide (AZO) coatings were measured and analyzed in the near infrared spectral region. The plain Drude model is the most simple model which can be used. However, it can describe the dielectric behavior of metals and semiconductors quite well at wavelengths exceeding the plasma edge if the degree of crystallinity and the amount of free charge carriers is high enough. The reflectances of conventional Sol-Gel ITO coatings with one to four layers and conventional Sol-Gel AZO coatings with seven to eleven layers were examined. The fit parameters which were obtained by modelling the measured reflectances are consistent and in good agreement with those found in literature.

Keywords: spectral reflectance, Drude model, tin doped indium oxide, aluminum doped zinc oxide

1 INTRODUCTION

Transparent conducting oxides (TCOs) combine physical material properties such as optical transparency and electrical conductivity, in order to provide spectrally selective characteristics or transparent electrodes [1]. Hence TCOs are used as coatings for energy-efficient windows [2], electrodes in flat-panel displays (LCD, OLED, PDP) [3], touch screens [4] and organic solar cells [5] for example. The most common and frequently used TCO coating is tin doped indium oxide (ITO) because of its high electrical conductivity and its high reflectance in the infrared spectral region combined with a high transmittance in the visible wavelength range. But the use of ITO is limited by the scarcity and high price of indium [6]. Therefore a good alternative TCO to ITO is needed. Aluminum-doped zinc oxide (AZO) is a promising candidate because it is inexpensive, non-toxic and exhibits sufficient infrared-optical and electrical properties [3].

In order to extend the comparison of the infrared-optical, electrical and structural performance of ITO and AZO conventional Sol-Gel coatings [7], the spectral reflectances of several ITO and AZO coatings were measured and fitted in the NIR region by using only the Drude model [1]. This model is a classical model which is

used to describe free electrons in any material. As the behavior of metals and semiconductors is essentially defined by free electrons, the dielectric behavior of such materials can be described by the Drude model quite well at wavelengths exceeding the plasma edge.

2 THEORETICAL MODEL

A more detailed description and derivation of the normal reflectance in the NIR spectral region by only using the Drude equations can be found in [1]. Therefore only the essential equations are shown. The Drude equations which describe the real part $\epsilon'(\omega)$ and the imaginary part $\epsilon''(\omega)$ of the dielectric function are given by [8]:

$$\epsilon'(\omega) = \epsilon_{\infty} \left(1 - \frac{N \cdot e^2}{(\omega^2 + \tau^{-2}) \cdot \epsilon_0 \cdot \epsilon_{\infty} \cdot m_{\text{eff}}} \right) \quad (1)$$

respectively

$$\epsilon''(\omega) = \frac{N \cdot e^2}{\omega \cdot \tau \cdot (\omega^2 + \tau^{-2}) \cdot \epsilon_0 \cdot m_{\text{eff}}} \quad (2)$$

The normal reflectance at the interface air / material can be described with the real part $n(\omega)$ and the imaginary part $k(\omega)$ of the complex refractive index and is given by the Fresnel equation [9]:

$$R(\omega) = \frac{(n(\omega) - 1)^2 + k(\omega)^2}{(n(\omega) + 1)^2 + k(\omega)^2} \quad (3)$$

The real and imaginary part of the complex refractive index are given by [1]

$$n(\omega) = \sqrt{\frac{\epsilon'(\omega) + \sqrt{\epsilon'(\omega)^2 + \epsilon''(\omega)^2}}{2}} \quad (4)$$

respectively

$$k(\omega) = \sqrt{\frac{-\epsilon'(\omega) + \sqrt{\epsilon'(\omega)^2 + \epsilon''(\omega)^2}}{2}} \quad (5)$$

By looking at these equations it can be seen that normal reflectances can be fitted by varying the high-frequency dielectric constant ϵ_{∞} , the scattering time τ and the quotient of the electron density N and the effective mass of the

electrons m_{eff} . There are only three fit parameters, because in equation (1) and (2) the electron density and the effective mass are always linked in the ratio N/m_{eff} so that an infinite number of different N and m_{eff} can form the same ratio of N/m_{eff} .

3 TCO COATINGS

The ITO and AZO coatings were processed by classical Sol-Gel processes and were deposited via dip-coating. The ITO Sol was prepared with indium nitrate, stannic chloride, acetylacetone and acetic acid dissolved in ethanol and acetone and the AZO Sol with zinc acetate dihydrate, aluminum nitrate nonahydrate and diethanolamine in isopropyl alcohol. The detailed preparation of these sols can be found in [7]. The doping concentration of the ITO Sol was 20 at% and the doping concentration of the AZO Sol was 0.75 at%.

A silica barrier layer with a thickness of about 200 nm has been deposited on the used soda-lime substrates and the ITO- respectively AZO-coatings were deposited onto the barrier layer, whereas the thickness of the individual wet-films can be controlled via the withdrawal speed [10]. After each layer deposition an interstage heating process was applied to the substrates and to gain a complete crystallization of the functional layers another final heat treatment was also applied. The detailed description of these heat treatments is published in [10] and [11].

By doping, which means substituting the trivalent indium atom with a tetravalent tin atom, and by producing oxygen defects in ITO layers, the layers can reach charge carrier concentrations up to 10^{21} cm^{-3} which are similarly to the charge carrier concentrations of metals [12]. AZO cannot be doped with that high doping concentration which are used with ITO because of the structure of the zinc oxide crystal [13]. Therefore by doping zinc oxide with aluminum atoms and producing oxygen defects charge carrier densities up to 10^{20} cm^{-3} can be reached [14]. To gain enough free electrons in AZO coatings to build a functional layer which has a similarly high reflectance like an ITO functional layer a lot more single layers of AZO have to be applied. Therefore AZO coatings with seven up to eleven single layers and ITO coatings with one to four single layers have been produced. Per layer the thickness of these Sol-Gel layers rises about approximately 100 nm, that means a four layered ITO coating has a thickness of about 450 nm and a eleven layered AZO coating has a thickness of about 1050 nm [7]. The thicknesses of all coatings are sufficient to avoid any contribution of the soda-lime glass to the measured reflectances. The investigated ITO and AZO layers are poly-crystalline and have a medium porosity with an average surface roughness of about 0.3 nm respectively 2.4 nm. The surface roughness of these layers is considerably smaller than the wavelength of the considered electromagnetic radiation and therefore these coatings show specular reflectance.

4 FITS OF THE MEASURED DATA

The normal hemispherical reflectance $R_{\text{nh}}(\omega)$ has been measured with the UV-VIS-NIR Spectrophotometer Lambda 950 in the wavelength range of $0.25 \mu\text{m} - 2.5 \mu\text{m}$ and with the FTIR spectrometer Bruker IFS 66v and the FTIR spectrometer Bruker Vector 22 in the range of $1.4 \mu\text{m} - 35 \mu\text{m}$. The fits have been performed and adjusted by using a least square method. The ITO and AZO Sol-Gel coatings which have been investigated exhibit a crystallinity, a charge carrier concentration and therefore an amount of free electrons which are a lot smaller than those of commercial sputtered TCO coatings. Also the slopes of the reflectance of Sol-Gel coatings are not as steep as the slope of the reflectances of sputtered TCO coatings [1]. Therefore the fits based on the plain Drude model can only describe the slope of the reflectances between $1.5 \mu\text{m}$ and $3.7 \mu\text{m}$ for ITO coatings and between $3.3 \mu\text{m}$ and $6.3 \mu\text{m}$ for AZO coatings [1]. But nevertheless the fits of the measured normal hemispherical reflectances provide fit parameters which are consistent and in a good agreement with those found in literature.

The measured and fitted normal hemispherical reflectance $R_{\text{nh}}(\lambda)$ of one to four layered ITO coatings are shown in Fig. 1.

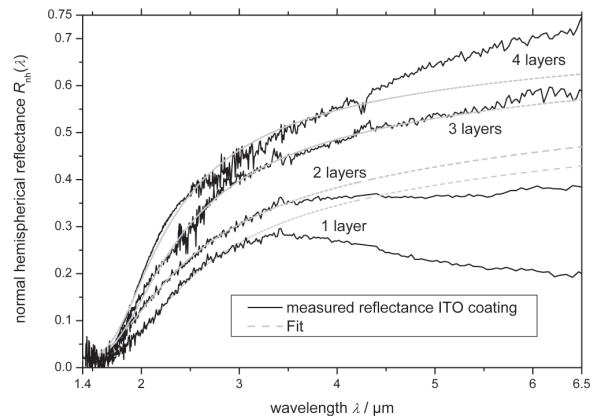


Figure 1: Measured and fitted normal hemispherical reflectance $R_{\text{nh}}(\lambda)$ of one to four layered ITO coatings.

The height of the reflectances of the ITO functional layers increases and their slopes get steeper with the increasing amount of single layers because of the growing number of free electrons in these layers. The reflectance of four single ITO coatings is the highest reflectance which can be realized, the reflectance of five single ITO layers is smaller than the reflectance of the four layered ITO coating [7]. For the sake of clarity, in Fig. 2 the measured and fitted normal hemispherical reflectance $R_{\text{nh}}(\lambda)$ of AZO coatings with seven and eleven layers in the spectral range from $3 \mu\text{m}$ to $35 \mu\text{m}$ and in Fig. 3 the reflectances of the eight, nine and ten layered AZO coatings are shown.

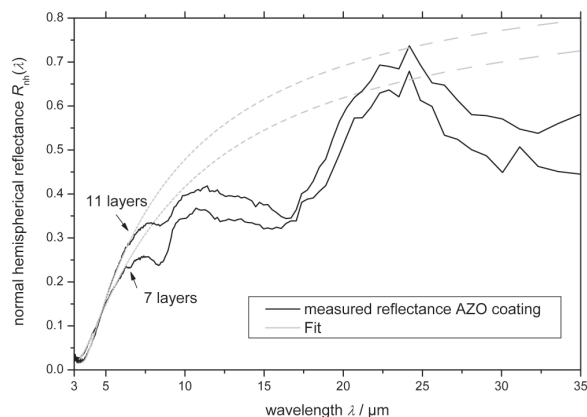


Figure 2: Measured and fitted normal hemispherical reflectance $R_{nh}(\lambda)$ of seven and eleven layered AZO coatings.

The reflectance of the AZO coatings also increases with an increasing number of single layers, but the heights and the slopes of the reflectances of these five different AZO layers differ not that much, therefore the data in Fig. 3 is presented in the wavelength range from 3 μm to 8.5 μm to gain an clearly arranged figure.

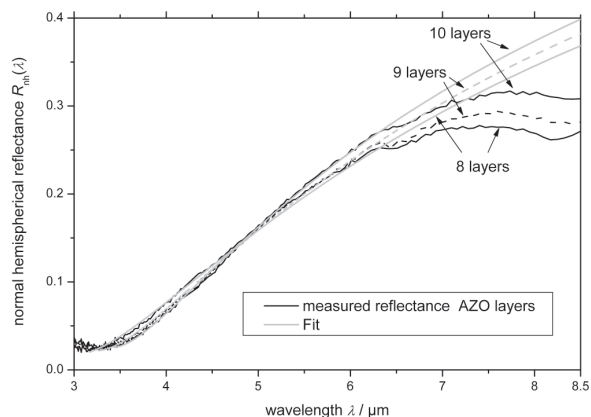


Figure 3: Measured and fitted normal hemispherical reflectance $R_{nh}(\lambda)$ of eight, nine and ten layered AZO coatings.

By looking at the graphs in Fig. 1, 2 and 3 it can be seen that the fits of the reflectances of AZO coatings always lie over the measured data. But only the fits of the reflectances of the one and two layered ITO coatings lie over the measured data, whereas the fits of the reflectances of the three and four layered ITO coatings lie below the measured data. This can be explained with the amount of free electrons within these TCO layers. If there are enough free electrons in TCO layers the fits lie under the measured data. Even the eleven layered AZO coating has a smaller amount of free electrons than the two layered ITO coating and therefore the slope of the eleven layered AZO coating

begins at higher wavelengths at about 3.4 μm , whereas the slope of the two layered ITO coatings begins at about 1.6 μm (see Fig. 4).

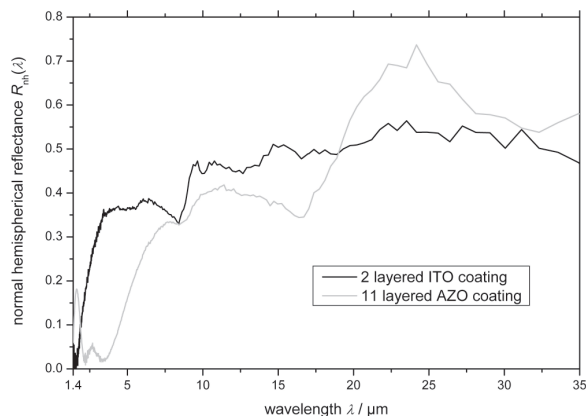


Figure 4: Measured normal hemispherical reflectance $R_{nh}(\lambda)$ of a two layered ITO coating and an eleven layered AZO coating.

The beginning of the slope correlates with the plasma wavelength $\lambda_p = 2\pi c \sqrt{\epsilon_0 \epsilon_\infty m_{eff}} / Ne^2$ which shifts to higher wavelengths if the charge carrier density N becomes smaller [15]. Fits based on the plain Drude model can describe the reflectance of coatings the better, the more free charge carriers are within the coatings.

5 DISCUSSION

In Table 1 the parameters obtained by the fits of the one to four layered ITO coatings and the expanded standard deviation of them are shown. The obtained values from these fits are consistent, that means the scattering time, the ratio of the effective mass of the electrons and the electron density and the dielectric constant of these four different ITO coatings are related as expected and are in a good agreement with those found in literature. The same is valid for the parameters obtained by the fits of the seven to eleven layered AZO coatings which are shown in Table 2. The expanded standard deviation of each fit parameter is also given in Table 2.

ITO coating	τ [fs]	$N / \frac{m_{eff}}{m_e} [10^{26} \text{ m}^{-3}]$	ϵ_∞
4 layers	2.24 ± 0.30	10.0 ± 1.7	2.9 ± 1.0
3 layers	2.06 ± 0.20	7.99 ± 0.40	2.41 ± 0.10
2 layers	1.70 ± 0.10	5.69 ± 0.10	1.68 ± 0.55
1 layer	1.64 ± 0.10	3.36 ± 0.10	1.28 ± 0.47

Table 1: Parameters obtained by the fits of the one to four layered ITO coatings.

Each fit parameter increases when the number of the TCO layers and therefore the number of free electrons increases. If the amount of free electrons rises, the charge carrier density also rises. The calculated effective mass of the ITO electrons is $0.34 m_e$ [16] and the calculated effective mass of AZO electrons lies in the range of $0.24 m_e$ [17] to $0.60 m_e$ [18]. This means that the charge carrier densities which are obtained by the fits of ITO are higher than the ones of AZO and lie in the areas which were mentioned above. The scattering time increases with the number of single layers because with the number of layers the amount of free charge carriers rises more than the amount of scattering centers and therefore the mean free path of the electrons increase. The scattering time of AZO coatings is bigger than the scattering time of ITO coatings because the AZO coatings have a significantly smaller doping concentration than ITO coatings. In literature scattering times in the range of 0.8 fs [19] and 12.6 fs [8] are reported. By looking at Table 1 and 2 it can be seen that the obtained scattering times are in a good agreement with the reported ones.

AZO coating	τ [fs]	$N \frac{m_{\text{eff}}}{m_e}$ [10^{26} m^{-3}]	ϵ_∞
11 layers	13.4 ± 5.2	3.80 ± 0.10	3.16 ± 0.20
10 layers	9.2 ± 2.4	3.51 ± 0.10	2.51 ± 0.10
9 layers	7.9 ± 2.1	3.20 ± 0.10	1.89 ± 0.10
8 layers	6.7 ± 2.3	2.97 ± 0.10	1.32 ± 0.10
7 layers	6.6 ± 2.0	2.80 ± 0.10	1.31 ± 0.10

Table 2: Parameters obtained by the fits of the seven to eleven layered AZO coatings.

The high-frequency dielectric constant of ITO and AZO is reported in literature in a range between 3 and 4 [20], [21]. The obtained high-frequency dielectric constants are therefore a little bit to small but in the same order of magnitude.

The fits and especially the obtained high-frequency dielectric constants could be improved by expanding the used model with the effective medium theory which takes the porosity of the coatings into account [1]. Besides the effective medium theory the presented fits could be improved by using the so called extended Drude model which takes an energy and frequency dependent scattering time into account [1].

6 CONCLUSION

It has been shown that the plain Drude model can be used to describe the slope of the normal hemispherical reflectance of ITO and also AZO coatings. The values obtained through these fits are consistent and in good agreement with those reported in literature.

REFERENCES

- [1] N. Wolf et al., J. Phys.: Conf. Ser. 395 012064 (2012)
- [2] R. G. Gordon, MRS Bulletin 25, 52–57, 2000
- [3] H. Wang et al., Rare Metals 29, 355–60, 2010
- [4] M. Grundmann et al, Phys. Status Solidi A 207, 1437–1449, 2010
- [5] K. Schulze et al., Appl. Phys. Lett. 91, 073521, 2007
- [6] S. Goldsmith et al., Thin Solid Films 517, 5146–5150, 2009
- [7] M. Rydzek, *Infrarot-optische, elektrische und strukturelle Charakteristika spektralselektiver Funktionsschichten auf der Basis dotierter Metalloxide*, PhD thesis (Würzburg) 2012
- [8] J. Davenas et al., Synthetic Metals 138, 295–8, 2003
- [9] R. Siegel, J. R: Howell, *Thermal Radiation Heat Transfer* vol 3 (USA: Hemisphere Publ. Corp.) 1992
- [10] M. Rydzek et al., Progress in Organic Coatings 70, 369–375, 2011
- [11] M. Reidinger et al., Thin Solid Films 517, 3096–3099, 2009
- [12] G. Kaune: *Röntgenografische Charakterisierung von ITO-Dünnschichten*, Diplomarbeit TU Chemnitz, 2005
- [13] P. Sagar et al., Vol.23, 685-696, 2005
- [14] V. Musat et al., Thin Solid Films 502, 219-222, 2006
- [15] M. Rydzek et al., High Temperatures - High Pressures, Vol. 38, pp. 277–293, 2009
- [16] A. Kurz: *Neue transparente elektrisch leitfähige Schichten, hergestellt durch nass-chemische Verfahren*, Dissertation an der Universität des Saarlandes, 2006
- [17] M. Oshikiri et al., Physica B: Condensed Matter, Volume 298, 472-476, 2001
- [18] Z. Qiao et al., Thin Sold Films 496, 520-525, 2006
- [19] H. Cachet et al., Thin Solid Films 388, 41-49, 2001
- [20] P.K. Biswas et al., Materials Letters 57, 2326–2332, 2003
- [21] Ü. Özgür et al., Journal of Applied Physics 98, 041301, 2005